

Scanning laser polarimetry in glaucoma

Tanuj Dada, Reetika Sharma, Dewang Angmo, Gautam Sinha, Shibal Bhartiya, Sanjay K Mishra, Anita Panda, Ramanjit Sihota

Glaucoma is an acquired progressive optic neuropathy which is characterized by changes in the optic nerve head and retinal nerve fiber layer (RNFL). White-on-white perimetry is the gold standard for the diagnosis of glaucoma. However, it can detect defects in the visual field only after the loss of as many as 40% of the ganglion cells. Hence, the measurement of RNFL thickness has come up. Optical coherence tomography and scanning laser polarimetry (SLP) are the techniques that utilize the evaluation of RNFL for the evaluation of glaucoma. SLP provides RNFL thickness measurements based upon the birefringence of the retinal ganglion cell axons. We have reviewed the published literature on the use of SLP in glaucoma. This review elucidates the technological principles, recent developments and the role of SLP in the diagnosis and monitoring of glaucomatous optic neuropathy, in the light of scientific evidence so far.

Key words: Fixed corneal compensation, glaucoma, retinal nerve fiber layer, scanning laser polarimetry

Access this article online

Website:
www.ijo.in

DOI:
10.4103/0301-4738.146707

Quick Response Code:



Glaucoma is an acquired progressive optic neuropathy characterized by changes in the optic nerve head and retinal nerve fiber layer (RNFL). White-on-white perimetry is the gold standard for diagnosis of glaucoma. Various new technologies are coming up for the early diagnosis of glaucoma. We performed a systemic search of the PubMed using the terms-glaucoma, scanning laser polarimetry (SLP), GDx and RNFL to prepare this review, which elucidates the technological principles, recent developments and the role of SLP in the diagnosis and monitoring of glaucomatous optic neuropathy.

Glaucoma and its Diagnosis: A Background

Imaging of RNFL is of vital importance in glaucoma as structural RNFL changes often precede functional visual field changes.^[1-3] As many as 40% of all ganglion cells can be lost before a well-defined scotoma is detected on the visual field.^[4] RNFL evaluation has been found to be more sensitive for predicting future visual field loss when compared to ONH evaluation and a better predictor of damage.^[5-10] Recent technology boom in ophthalmology has given us two technologies that are capable of providing highly reproducible RNFL assessments. Optical coherence tomography (OCT) based on low-coherence interferometry, generates posterior segment thickness measurements with an axial resolution of eight to ten microns while SLP provides RNFL measurements based upon the birefringence of the retinal ganglion cell axons.

Technologic Principle

Retinal nerve fiber layer is made of highly ordered parallel axon bundles which contain microtubules, cylindrical intracellular organelles with diameters smaller than the wavelength of light. The paralleled structure of the microtubules is the source of RNFL birefringence that is the splitting of a light wave by a polar material into two components. These components travel at different velocities that create a relative phase shift termed "retardation". This retardation is proportional to the thickness of the RNFL.^[11,12] Total retardation of a subject's eye is the sum of cornea, lens, and RNFL birefringence. Compensation of anterior segment birefringence is thus necessary to isolate RNFL birefringence.

Scanning laser polarimetry is basically a confocal scanning laser ophthalmoscope with an integrated ellipsometer to measure retardation. It determines the RNFL thickness, point by point in the peripapillary region, by measuring the total retardation in the light reflected from the retina. Polarized light passes through the eye and is reflected off the retina.^[13-16] Because the RNFL is birefringent, the two components of the polarized light are phase shifted relative to each other and this is captured by a detector, and converted into thickness (in microns).^[11]

Generations of Scanning Laser Polarimetry and Calculation of Birefringence

Fixed corneal compensation

The first-generation device (nerve fiber analyzer [NFA] I) became commercially available in 1992 and was equipped with a single detector, which was later replaced by a double detector (NFA II). These earlier versions of SLP (e.g. the GDx NFA, GDx Access) were compensated for anterior segment birefringence based on fixed values for the axis and magnitude of the anterior segment birefringence. However, later it was found that the axis and magnitude are variable

Dr. Rajendra Prasad Centre for Ophthalmic Sciences, All India Institute of Medical Sciences, New Delhi, India

Correspondence to: Dr. Tanuj Dada, Dr. Rajendra Prasad Centre for Ophthalmic Sciences, All India Institute of Medical Sciences, New Delhi, India. E-mail: tanujdada@gmail.com

Manuscript received: 05.07.14; Revision accepted: 03.11.14

for each individual and using a fixed corneal compensation may not adequately account for the aforementioned variables.^[17]

Variable corneal compensation

In 2002, variable corneal compensation (VCC) was introduced, allowing eye-specific compensation of anterior segment birefringence, commercially available in the 5th iteration of the SLP instrument named GDx-VCC (Carl Zeiss Meditec, Inc., Dublin, California, USA).

GDx-VCC measures and individually compensates for anterior segment birefringence, using a 780–790 nm laser diode.^[14–16] The axis of the anterior segment birefringence is determined by the orientation of the 'bow-tie' birefringent pattern [Fig. 1] in the macula and the magnitude of the anterior segment birefringence is calculated by analyzing the circular profile of the birefringence in the macula according to standard equations.^[11] In cases of macular pathology, an alternative method is available that accurately compensates for the anterior segment birefringence.^[18]

GDx-Enhanced corneal compensation

The enhanced corneal compensation (ECC) algorithm is implemented in the GDx-VCC by a software modification. A known birefringence bias is introduced into the measurement beam path to shift the measurement of total retardation into a more sensitive region of the curve of detection of polarization of the instrument. The bias retarder is formed by the combination of the variable corneal compensator and cornea. However, instead of completely canceling corneal birefringence, the retarder is adjusted and hence that the combination has retardance close to 55 nm and slow axis of polarization close to vertical. After image acquisition, the birefringent bias is removed mathematically, point-by-point, to yield the RNFL retardation values that are converted to thickness (in micrometers) using a fixed conversion factor.

The computerized export of the temporal-superior-nasal-inferior-temporal (TSNIT) plots on the GDx-ECC printout includes the mean RNFL thickness from 64 polar sectors (5.625°/arc). The mean for each sector is computed along the 3.2 mm diameter measurement circle surrounding the optic nerve head. The mean RNFL thickness for the superior (0–180°)

and inferior (181–360°) retinal region is computed separately. ECC scans show a stronger structure-function relationship with perimetry compared with VCC.^[19,20]

Modified diameter scan

GDx-VCC uses a fixed scan circle of 3.2 mm diameter centered on the optic disc (conventional diameter scan). This may be affected by peripapillary atrophy (PPA). So it has measurement options with two additional scan diameters – medium and large. Dada *et al.*^[21] found that medium and large diameter scans can also be used to discriminate between normal and glaucomatous eyes. Nerve fiber indicator (NFI) has been seen to be the best discriminating parameter across all diameters.

Retinal nerve fiber layer measurements

The GDx-VCC measurements are taken by scanning the beam of a near-infrared laser (780 nm) in a raster pattern^[12] which captures an image with a field 40° horizontally by 20° vertically, and including both the peripapillary and the macular region.^[22] It generates two images: A reflectance image and a retardation image [Fig. 2]. Each image is made up of 256 (horizontal) × 128 (vertical) pixels, or 32,768 total pixels. For an emmetropic eye, 1 pixel is 0.0465 mm in size, and the total scan field is 11.9 mm (horizontal) × 5.9 mm (vertical).^[23]

Clinical Interpretation of the GDx Printout

For each GDx-VCC scan, an age-matched comparison is made to the normative database, and any significant deviations from normal limits are flagged as abnormal with a 'P' value. Quantitative RNFL evaluation is provided through four key elements of the printout [Fig. 3]:

- Thickness map
- Deviation map
- TSNIT graph [Fig. 4a and b]
- Parameter table [Fig. 5].

Nerve fiber indicator

The NFI is a global measure based on the entire RNFL thickness map. NFI ranges from 1 to 100, with lower values (<25) indicating a normal RNFL.^[24–27]

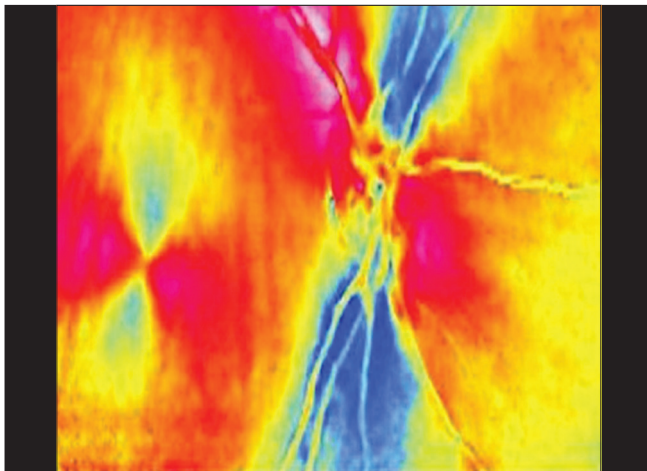


Figure 1: "Bow-tie pattern" (arrow) seen in the macula in an uncompensated scan

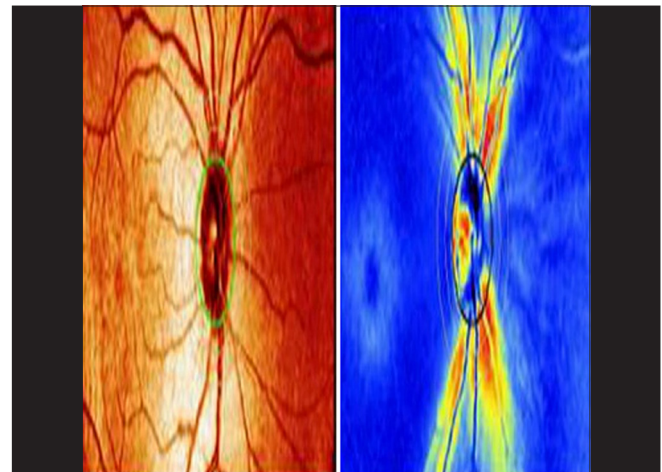


Figure 2: Images generated by the GDx-variable corneal compensation: Left image is the reflectance image displayed as a colored intensity map. The right image is the retardation map converted to retinal nerve fiber layer thickness, color coded based on the color spectrum

Clinical applications

Scanning laser polarimetry technology can help in early diagnosis of glaucoma by picking up RNFL changes that may precede visual field damage by 5–6 years [Table 1].

Healthy subjects

Age has been found to significantly affect all RNFL measurements with the ECC protocol of SLP, whereas typical scan score (TSS) and residual anterior segment retardance affect the overall average and the superior average RNFL measurements, respectively.^[28]

Glaucoma suspect

Medeiros et al.^[29] found GDx-VCC to be superior versus Heidelberg retina tomograph 3 (HRT3) for detecting early damage in glaucoma suspects. They studied 82 glaucoma suspects. The area under the receiver operator characteristic (AUROC) curve for the best parameter from GDx-VCC (NFI) was significantly larger than that of the best parameter from the HRT (rim volume) (0.83 vs. 0.70).

Mohammadi et al.^[30] studied one eye from each of 160 glaucoma suspects with normal standard automated perimetry (SAP) visual fields. They found thinner baseline SLP RNFL measurements to be independent predictors of future visual field damage.

Badalà et al.^[31] in their study compared OCT, GDx-VCC, HRT and stereophotographs in 46 healthy subjects and 46

glaucoma patients with early defect. The largest AUROC for each technique was 0.96 for OCT average thickness, 0.92 for GDx-VCC NFI, 0.91 for HRT3 FSM discriminant function and 0.97 for stereophotographs.

Shaikh et al.^[32] studied 39 “glaucoma suspects.” Twenty-two of 39 (56.4%) were considered to be at risk of developing progressive glaucoma. In 19 of these patients, abnormal GDx-VCC results were found, particularly inter-eye asymmetry in the RNFL thickness. However, in two of 39 (5.1%) patients the GDx-VCC was normal, despite the presence of a neuroretinal rim defect in the optic disc with corresponding visual field loss, and in one patient with POAG. Hence, they concluded that GDx-VCC should not be used in isolation.

Li et al. found NFI to be the best performing parameter using a cutoff of 35 with a sensitivity of 75%, specificity of 95%, a positive predictive value of 25 and a negative predictive value of 99 for diagnosing glaucoma.^[33]

In a study to assess the relationship between high-definition OCT (HD-OCT) and SLP with VCC and ECC in measuring RNFL in healthy eyes and those with early-to-moderate glaucomatous VF loss, HD-OCT parameters of RNFL thickness were found to be significantly higher than VCC and ECC parameters, and therefore those thickness values are not interchangeable in normal eyes and in early glaucoma patients.^[34]

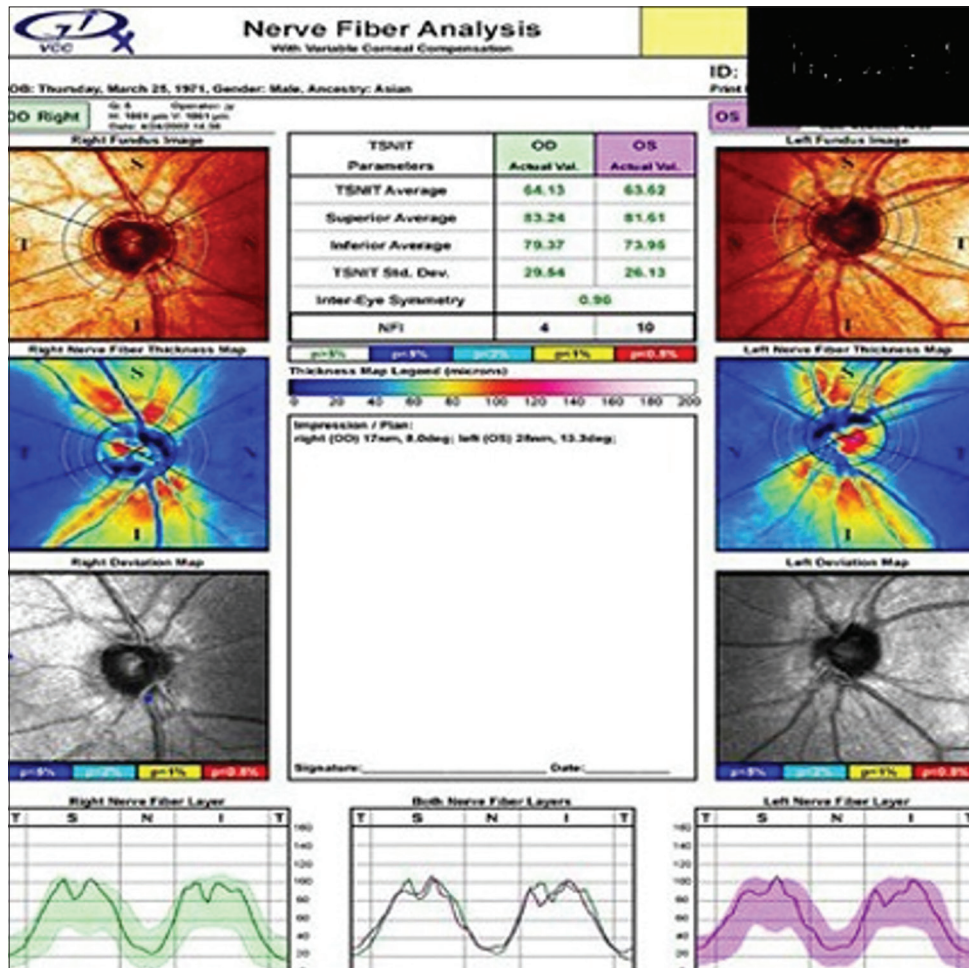


Figure 3: Print out showing various parameters for quantitative retinal nerve fiber layer evaluation

Table 1: Summary of studies using GDx in glaucoma management

Study	Number of participants	Type of participants	Modality used	Results
Glaucoma suspects				
Medeiros <i>et al.</i> ^[29]	82	Glaucoma suspects	GDx HRT	Area under the receiver operating characteristic: NFI: 0.83 Rim volume: 0.70 Glaucoma probability score: 0.68
Mohammadi <i>et al.</i> ^[30]	160	Glaucoma suspects	GDx	Thinner baseline SLP RNFL measurements were independent predictors of future visual field defect
Badalà <i>et al.</i> ^[31]	46 46	Normal Glaucoma suspects	Stratus OCT, GDx-VCC, HRT3, stereoscopic optic disc photographs	Stratus OCT: 0.96 GDx-VCC NFI: 0.92 HRT3 FSM discriminant function 0.91 Stereo photographs: 0.97
Shaikh and Salmon ^[32]	39	Glaucoma suspects	GDx-VCC Full ophthalmological examination	19 of 22 patients found to be at risk had abnormal GDx-VCC
Early glaucoma				
Zheng <i>et al.</i> ^[35]	40 normal 80 early glaucoma 70 advanced glaucoma	Normal and glaucoma patients of various degrees	GDx-VCC	Area under the receiver operating characteristic > 0.70 NFI and inferior average: 0.81
Da Pozzo <i>et al.</i> ^[36]	62 48	Normal Glaucoma patients	GDx-VCC	Area under the receiver operating characteristic for NFI=0.870 Superior average: 0.817 Normalized superior area: 0.816
Parikh <i>et al.</i> ^[37]	104 74	Normal Glaucoma	GDx-VCC	TSNIT standard deviation Sensitivity: 61.3 Specificity: 95.2 NFI: >50 Sensitivity: 52.7% Specificity: 99% Positive predictive values: 74.3% Negative predictive values: 97.6%
Moderate to severe glaucoma				
Reus and Lemij ^[39]	77 162	Normal Glaucoma patients	GDx-VCC	Area under the receiver operating characteristic: 0.90-0.98
Ocular hypertension				
Henderson <i>et al.</i> ^[40]	48 44	Normal OHT	CCT GDx-VCC	Patients with thinner corneas had significantly thinner RNFL values than those with thicker corneas and healthy control subjects
Normal tension glaucoma				
Choi <i>et al.</i> ^[41]	43 56	Normal NTG	GDx-VCC	Perimetrically normal hemifields of NTG eyes showed significantly lower RNFL thickness parameters than the corresponding retinal regions of healthy eyes
JOAG				
Zareii <i>et al.</i> ^[43]	24 24	Normal JOAG	GDx-VCC	Area under the receiver operating characteristic: GDx VCC: NFI=0.99 OCT (inferior average) =0.92

JOAG: Juvenile open angle glaucoma, HRT: Heidelberg retina tomograph, NFI: Nerve fiber indicator, OCT: Optical coherence tomography, VCC: Variable corneal compensation, NTG: Normal tension glaucoma, RNFL: Retinal nerve fiber layer, TSNIT: Temporal-superior-nasal-inferior-temporal, SLP: Scanning laser polarimetry, FSM: Frederick S. Mikelberg

Early glaucoma

According to Zheng *et al.*,^[35] NFI and inferior average are the most effective indicators for the early diagnosis of glaucoma. AUROCs were 0.81 for NFI and inferior average with better differentiation capability.

Da Pozzo *et al.*^[36] evaluated the diagnostic accuracy of GDx-VCC comparing 62 healthy and 48 glaucomatous age-matched patients with early glaucomatous field defect. The three parameters with largest AUROCs were NFI (0.870), superior average (0.817) and normalized superior area (0.816).

Parikh *et al.*^[37] evaluated 74 eyes with early glaucoma and 104 eyes of normal subjects. TSNIT SD had the best combination of sensitivity and specificity-61.3 and 95.2, respectively-followed by NFI > 50 (sensitivity, 52.7%; specificity, 99%).

Fortune *et al.* in their study found that the onset of progressive loss of RNFL retardance occurs earlier than the onset of RNFL thinning. Endpoints of progressive loss from baseline also occurred more frequently and earlier for RNFL retardance as compared with a thickness.^[38]

Moderate-to-severe glaucoma

Reus and Lemij^[39] compared 77 healthy eyes and 162 glaucomatous patients. AUROC for main GDx-VCC parameters ranged from 0.90 to 0.98.

Ocular Hypertension

Henderson *et al.*^[40] studied 44 ocular hypertension (OHT) patients and 48 healthy subjects, all of similar age. Higher NFI scores were correlated significantly with thinner CCT measurements in OHT patients. In multivariate analysis, only age and CCT measurement were associated significantly with RNFL measurements in OHT eyes.

Normal tension glaucoma

Choi *et al.*^[41] evaluated RNFL in the retinal segments without visual field loss in eyes with 56 Asian normal tension glaucoma (NTG) patients who had localized visual field defects confined to 1 hemifield and 43 normal controls. They found that perimetrically normal hemifields of NTG eyes had significantly lower RNFL thickness parameters than the corresponding regions of healthy eyes.

Normal tension glaucoma versus high tension glaucoma

Jung *et al.*^[42] found GDx-VCC to be more sensitive in detecting RNFL damage in high tension glaucoma (HTG) patients compared to NTG patients. Compared with eyes with NTG, eyes with HTG showed reduced RNFL thickness.

Juvenile Open-Angle Glaucoma

Zareii^[43] compared the ability of GDx-VCC and OCT to discriminate eyes with Juvenile Open-Angle Glaucoma from

normal eyes. They observed statistically significant correlations between the two. The greatest AUROC parameter on OCT (inferior average: 0.92) had a lower area than that in GDx-VCC (NFI: 0.99).

Exfoliation syndrome

Dimopoulos *et al.*^[44] compared RNFL thickness of normotensive eyes with exfoliation syndrome (XFS) and healthy eyes using GDx-VCC. Polarimetry-determined RNFLT was lower in XFS eyes with normal IOP. Therefore, close monitoring of RNFLT may facilitate early identification of those XFS eyes that convert to exfoliative glaucoma.

Detecting Progression

The new software used in GDx that helps in investigating progression is GPA™ (progression analysis for GDx) [Fig. 6]. The GDx-GPA algorithms are designed to have 95% specificity for “Likely progression.”

GDx-GPA uses two different algorithms:

- Change from baseline (CFB): Based on changes from two baseline exams compared to measurement variability
- Statistical image mapping: Based on trend analysis. All visits contribute to change detection here in contrast to CFB where data from the first two and last two visits are used.

Atypical Retardation Patterns

Atypical retardation patterns (ARPs) have been characterized as irregular patches of elevated retardation values that are against the expected retardation distribution based on the RNFL anatomy.^[45] ARPs may provide fallacious RNFL measurements^[46] and occur in approximately 10–25% of healthy eyes and 15–51% of glaucomatous eyes,^[45,47,48] in elderly subjects,^[49] in lightly pigmented fundi and in high myopes. SLP images are generally excluded from the analysis when the software flags them as incompatible with its normative database. The software flags an image as such when the TSS is below 25.^[50]

Typical scan score

TSS is a proprietary measure provided by the GDx-VCC software that indicates whether the observed retardation pattern is typical of the human healthy or glaucomatous

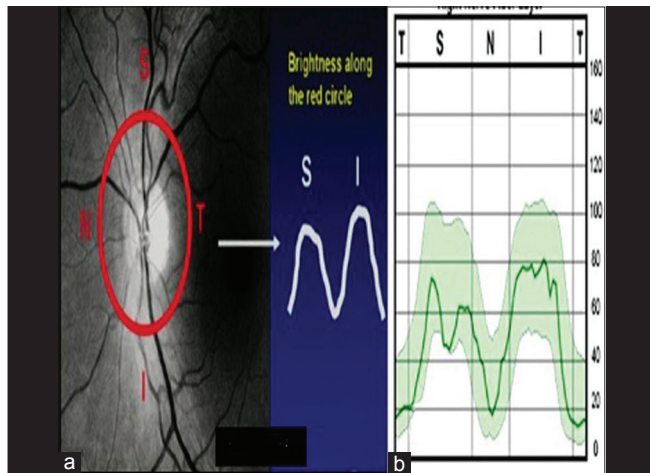


Figure 4: (a and b) Calculation circle, characteristic double hump pattern

TSNIT Parameters	OD Actual Val.	Actual Val.
TSNIT Average	48.08	33.27
Superior Average	54.39	46.23
Inferior Average	62.33	28.06
TSNIT Std. Dev.	22.36	14.83
Inter-Eye Symmetry	0.50	
NFI	25	63

Figure 5: Temporal-superior-nasal-inferior-temporal parameters

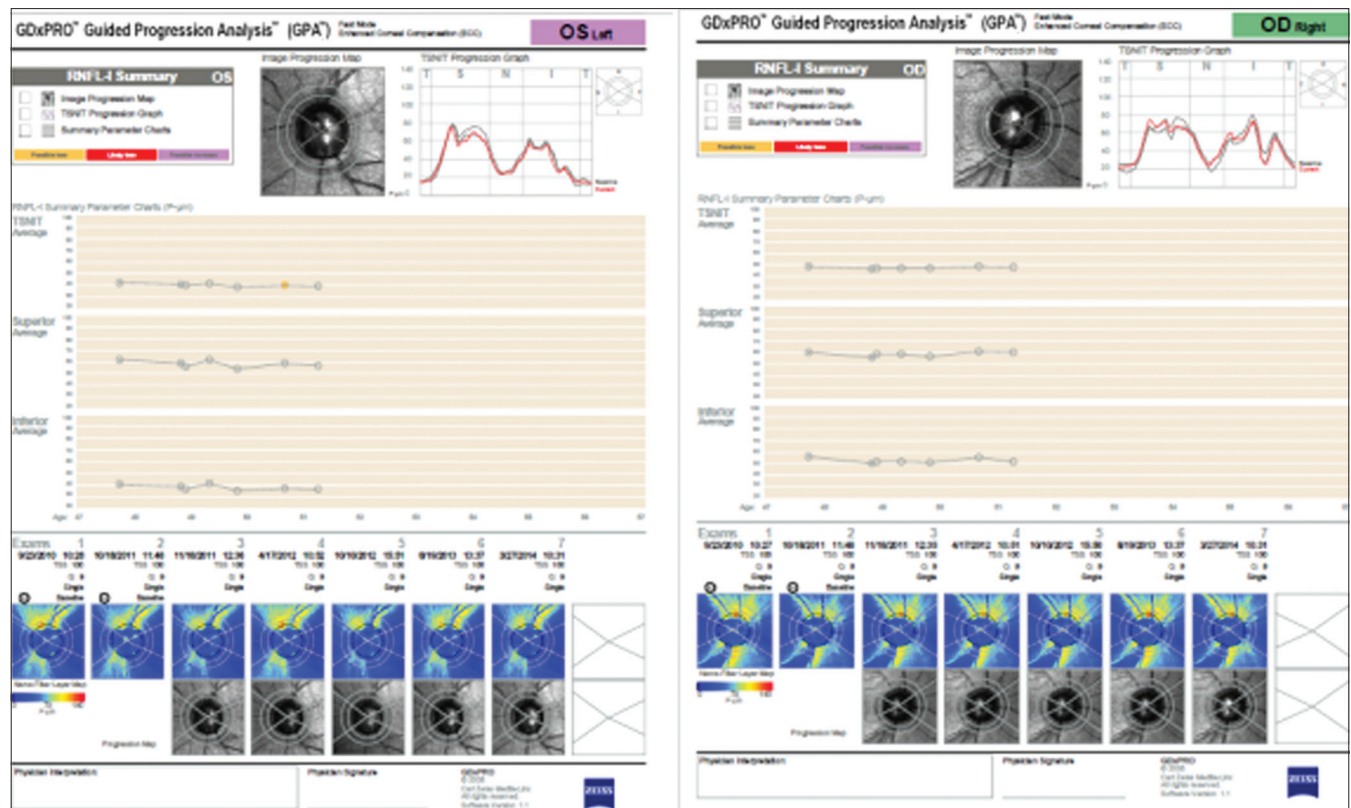


Figure 6: Overview of progression analysis using GPA software

RNFL (range: 0–100). In scans that display an ARP, the TSS is lower. It is highly predictive of the presence of ARPs.^[47] In clinical studies, a cut-off value for TSS of 80 is often used to discriminate between normal and atypical retardation patterns.^[45,51,52] The ability of SLP to discriminate between healthy and glaucomatous eyes has been shown to decrease when ARPs are present.^[46–48] Diagnostic accuracy has been found to be comparable for SD-OCT and GDx-VCC if typical scans (TSS = 100) are investigated.^[53] Decreasing TSS is associated with a decrease in diagnostic accuracy for discriminating healthy and glaucomatous eyes by SLP. NFI has been found to be less influenced than the global or sector RNFL thickness. GDx ECC helps in the neutralization of ARPs.

Wang *et al.* evaluated the changes of visual field and RNFL during 24 months follow-up in primary open-angle glaucoma (POAG) patients. Visual field and RNFL were detected by using GDx-VCC system and Octopus perimeter in 60 patients with POAG in early stage (60 eyes), 32 in moderate stage (32 eyes) and 30 in advanced stage (30 eyes). They found GDx-VCC system to be useful to evaluate the progression of POAG in early and moderate stage by detecting the change of the RNFL thickness with long-term follow-up.^[54]

In a study by Medeiros *et al.*^[55] 213 eyes of 213 patients with an average follow-up time of 4.5 years were studied annually with the ECC and VCC, along with optic disc stereophotographs and SAP. Thirty-three patients (15%) showed progression over time on visual fields and/or stereophotographs. Mean rates of average RNFL thickness change measured by the GDx-ECC were significantly different in progressors versus nonprogressors ($-1.24 \mu/\text{year}$ vs. $-0.34 \mu/\text{year}$;

$P < 0.001$). AUROC curve for discriminating progressors from nonprogressors was significantly higher for rates of change measured by ECC compared to VCC (0.89 vs. 0.65; $P < .001$). Rates of RNFL change detected by the GDx ECC were significantly greater in eyes with progressive glaucoma compared to eyes with stable disease. Also, the ECC performed significantly better than the VCC for detection of change.

Makabe *et al.*^[56] also found that longitudinal progression in NFI obtained with GDxVCC was significantly correlated with that in Humphrey field analyzer humphrey field analyzer (HFA) parameters, such as mean deviation and pattern standard deviation and recommended that GDx-VCC is a useful tool for longitudinal follow-up assessment of glaucoma.

Special Scenarios

Effect of cataract surgery

Scanning laser polarimetry measures the shift in polarization of light that is associated with the natural birefringence of RNFL. Other birefringent structures within the eye include cornea and lens. The GDx compensates for the birefringence of the cornea in part but that caused by lens is not compensated and hence there can be change in RNFL thickness after cataract surgery.

Vetrugno *et al.*^[57] examined 68 eyes of 68 patients undergoing phacoemulsification with foldable intraocular lens (IOL) implantation (silicone and acrylic) by SLP before and after surgery. They could not find any statistically significant difference between SLP parameters before and after cataract surgery, regardless of the type of IOL implanted.

In contrast to this, Park *et al.*,^[58] Iacono *et al.*^[59] and Dada *et al.*^[60] stressed on new baseline SLP measurements after cataract extraction with IOL. Gazzard *et al.*^[61] have also shown a significant change in SLP measurements after cataract extraction, especially in patients with posterior subcapsular cataract.

Brittain *et al.*^[62] investigated changes in GDx-VCC parameters caused by posterior capsular opacification. Typical scan score significantly improved after laser from 33 to 55.1 ($P = 0.001$; $n = 19$) and TSNIT score was significantly lower, dropping from 62.3 to 58.9 ($P = 0.03$; $n = 19$).

Effect of refractive surgery (laser in situ keratomileusis (LASIK), photo refractive keratectomy)

Dada *et al.*^[63] and Zangwill *et al.*^[64] could not find any statistically significant change in any of the parameters of RNFL before and after LASIK. Katsanos *et al.*,^[65] however, found transient changes in RNFL by SLP after LASIK, which became stable by the 3rd postoperative month.

Comparison with other Diagnostic Modalities

Scanning laser polarimetry versus optical coherence tomography

Leung *et al.*,^[66] Chung^[67] and Kim *et al.*^[68] have reported that the total average RNFL thickness measured with Stratus OCT and GDx-VCC were highly correlated. Yoo *et al.*^[69] found that overall performance of Stratus OCT and GDx-VCC about their internal normative database was not significantly different.

Aptel *et al.*^[70] tested 120 eyes of 120 patients (40 with healthy eyes, 40 with suspected glaucoma, and 40 with glaucoma) on Cirrus-OCT, GDx-VCC, and SAP. With spectral-domain OCT, the correlations ($r(2)$) between RNFL thickness and visual field sensitivity ranged from 0.082 to 0.726. By comparison, with GDx-VCC, the correlations ranged from 0.062 to 0.362. The largest AUROC were seen for OCT superior thickness (0.963 ± 0.022 ; $P < 0.001$) in eyes with glaucoma and for OCT average thickness (0.888 ± 0.072 ; $P < 0.001$) in eyes with suspected glaucoma. They concluded that the structure-function relationship was significantly stronger with OCT than with GDx-VCC.

Lee *et al.*^[71] found AUROCs of the Cirrus OCT to be significantly higher than those of GDx-VCC in glaucoma detection. The best-performing parameter was the NFI in GDx-VCC and inferior RNFL thickness in cirrus-OCT (AUROC = 0.912, 0.961, $P = 0.045$). There was good agreement between the two instruments with respect to abnormal classifications (κ , 0.611–0.766).

Xu *et al.*^[72] investigated the performance of SDOCT and SLP to detect progressive RNFL changes in glaucoma and found that at a comparable level of specificity, progressive RNFL thinning was detected more often than progressive reduction of retardance.

Bagga *et al.*^[47] showed that images with ARPs have a weaker correlation with RNFL thickness measured with OCT compared with images with normal patterns. These results were subsequently confirmed in a study by Sehi *et al.*^[73]

Garas^[74] found that the diagnostic accuracy of the GDx-VCC/ECC NFI and RTVue-OCT average RNFLT were similar in glaucoma cases.

Schallenberg *et al.*^[75] used GDx-VCC, GDx-ECC, and Spectralis-OCT to study RNFL measurements in 92 eyes of 92 glaucoma patients with various amount of glaucomatous damage and found that they cannot be directly compared because of differences in method of the devices.

Scanning Laser Polarimetry Versus Frequency Doubling Technology/Standard Automated Perimetry

In the Groningen Longitudinal Glaucoma Study^[76] seventy glaucoma suspect patients with normal test results at baseline were followed prospectively for 4 years with SAP, frequency doubling technology and GDx. Conversion of suspects was better picked up by GDx.

Scanning laser polarimetry versus Heidelberg retina tomograph

Alencar *et al.*^[77] found that the measurements of rates of change in GDx-VCC RNFL thickness were superior to HRT Rim area in identifying eyes with progression.

Kanamori *et al.*^[78] also found GDx-VCC, HRT and OCT to be useful in preperimetric and early glaucoma. In their study of glaucomatous eyes with or without early visual field defects, SLP and OCT performed similarly or had better discriminating abilities compared with CSLO.

Medeiros *et al.*^[79] compared the GDx-VCC, the HRT II and the Stratus OCT best parameters (NFI, the linear discriminant function and Inferior Average, respectively) in their ability to discriminate healthy eyes from glaucomatous patients. The AUROC curve of the three parameters indicated excellent discriminating power, without significant differences between them. For the GDx-VCC the three best performing parameters were NFI (0.91), Normalized Inferior Area (0.86) and TSNIT average (0.85).

Scanning Laser Polarimetry Versus Matrix Perimetry, Optical Coherence Tomography, and Retinal Nerve Fiber Layer Photography using Heidelberg Retina Angiograph 1

Hong *et al.*^[80] compared the efficacy of detecting early glaucoma using all these in 72 POAG patients with early-stage visual field defects and 48 healthy controls. The AUROCs of Matrix perimetry, GDx-VCC, OCT, and RNFL photography using Heidelberg retina angiograph 1 with the best discriminating parameter were 0.990, 0.906, 0.794, and 0.751, respectively.

Strengths of Scanning Laser Polarimetry

Scanning laser polarimetry is a sophisticated technology that provides highly reproducible, objective measurements of the peripapillary RNFL. It is easy to operate, does not require pupillary dilatation, is highly reproducible, does not employ a reference plane, does not require correction for ocular magnification and incorporates an age-matched normative database. GDx-ECC has largely reduced ARP and is capable

of neutralizing any residual anterior segment birefringence not completely compensated by VCC.

Retinal nerve fiber layer Integrity™

The RNFL-I measurement is the phase shift that occurs when polarized light passes through the RNFL. SLP captures birefringence, a tissue property that depends on the integrity of retinal ganglion cell axon microtubules and neurofilaments and hence SLP has the capacity not only to corroborate findings of RNFL thinning as determined by other methods, but may also provide insight into structural damage due to changes in density and orientation of the RNFL microstructures that may precede or occur in the absence of RNFL thinning.

Limitations

Peripapillary atrophy

Image quality may be compromised if PPA falls under the measurement circle. Kunimatsu *et al.*^[81] found reproducibility of GDx parameters to be similar among three circles in normal eyes ($P > 0.05$), whereas coefficients of reproducibility of TSNIT average ($P = 0.006$) and superior average ($P = 0.035$) were smaller in the smaller circles in OAG eyes. They recommended using medium circles in OAG patients as the obstructing influences of PPA on GDx measurement could be avoided.

Refractive error

Manufacturer recommendation is to avoid scans in eyes with refraction outside the + 5/-10 spherical diopter range as the probability of obtaining low-quality scans increases markedly. Patients wearing contact lenses can undergo GDx-VCC. Wang *et al.*^[82] found that the average RNFL thickness measured with Cirrus HD-OCT decreases as the degree of myopia increases while no such correlation was detected in GDx-ECC. Wang *et al.*^[83] in another study found RNFL thickness to be lower in all but the nasal quadrant in patients with POAG and high myopia (HM), compared to patients with only HM. GDx-VCC was found to be better than OCT in detecting POAG in HM patients. Dada *et al.*^[84] studied RNFL thickness in myopia with SLP. Moderate myopes showed a significant thinning of the RNFL. In HM due to PPA and contribution of scleral birefringence, the RNFL values were abnormally high.

Tilted disc

Yu *et al.*^[85] and Bozkurt *et al.*^[86] have reported GDx to be unreliable in tilted disc.

Macular pathology

A large area centered on the fovea ($6^\circ \times 6^\circ$ square region) should be used in macular pathology.^[87] Dada *et al.*^[88] studied the effect of two macular birefringence protocols (bow-tie retardation and irregular macular scan) using GDx-VCC on RNFL thickness parameters and found the standard protocol to overestimate RNFL thickness in eyes with macular lesion which was normalized using the irregular macular pattern protocol.

Conclusion

GDx-VCC has emerged as a valuable, objective tool of clinical value in the management of glaucoma. GDx-ECC has overcome the presence of ARPs and improved the diagnostic accuracy and the relationship between functional and structural measurements. It is useful for early detection of structural

damage to RNFL and longitudinal follow-up to pick up progression. However the clinician should be aware of its limitations, reconfirm an abnormal test, check the image quality and always use the GDx test report in conjunction with clinical evaluation of the optic nerve head and functional testing for starting or adjusting glaucoma therapy.

References

1. Sommer A, Katz J, Quigley HA, Miller NR, Robin AL, Richter RC, *et al.* Clinically detectable nerve fiber atrophy precedes the onset of glaucomatous field loss. *Arch Ophthalmol* 1991;109:77-83.
2. Sommer A, Miller NR, Pollack I, Maumenee AE, George T. The nerve fiber layer in the diagnosis of glaucoma. *Arch Ophthalmol* 1977;95:2149-56.
3. Caprioli J, Prum B, Zeyen T. Comparison of methods to evaluate the optic nerve head and nerve fiber layer for glaucomatous change. *Am J Ophthalmol* 1996;121:659-67.
4. Quigley HA, Addicks EM, Green WR. Optic nerve damage in human glaucoma. III. Quantitative correlation of nerve fiber loss and visual field defect in glaucoma, ischemic neuropathy, papilledema, and toxic neuropathy. *Arch Ophthalmol* 1982;100:135-46.
5. Quigley HA, Katz J, Derick RJ, Gilbert D, Sommer A. An evaluation of optic disc and nerve fiber layer examinations in monitoring progression of early glaucoma damage. *Ophthalmology* 1992;99:19-28.
6. Airaksinen PJ, Alanko HI. Effect of retinal nerve fibre loss on the optic nerve head configuration in early glaucoma. *Graefes Arch Clin Exp Ophthalmol* 1983;220:193-6.
7. Quigley HA. Examination of the retinal nerve fiber layer in the recognition of early glaucoma damage. *Trans Am Ophthalmol Soc* 1986;84:920-66.
8. Quigley HA, Enger C, Katz J, Sommer A, Scott R, Gilbert D. Risk factors for the development of glaucomatous visual field loss in ocular hypertension. *Arch Ophthalmol* 1994;112:644-9.
9. Jonas JB, Hayreh SS. Localised retinal nerve fibre layer defects in chronic experimental high pressure glaucoma in rhesus monkeys. *Br J Ophthalmol* 1999;83:1291-5.
10. Zhou Q, Weinreb RN. Individualized compensation of anterior segment birefringence during scanning laser polarimetry. *Invest Ophthalmol Vis Sci* 2002;43:2221-8.
11. Weinreb RN, Dreher AW, Coleman A, Quigley H, Shaw B, Reiter K. Histopathologic validation of Fourier-ellipsometry measurements of retinal nerve fiber layer thickness. *Arch Ophthalmol* 1990;108:557-60.
12. Morgan JE, Waldock A, Jeffery G, Cowey A. Retinal nerve fibre layer polarimetry: Histological and clinical comparison. *Br J Ophthalmol* 1998;82:684-90.
13. Dreher AW, Reiter K. Retinal laser ellipsometry: A new method for measuring the retinal nerve fiber thickness distribution. *Clin Vision Sci* 1992;7:481-8.
14. Weinreb RN, Bowd C, Zangwill LM. Glaucoma detection using scanning laser polarimetry with variable corneal polarization compensation. *Arch Ophthalmol* 2003;121:218-24.
15. Medeiros FA, Zangwill LM, Bowd C, Bernd AS, Weinreb RN. Fourier analysis of scanning laser polarimetry measurements with variable corneal compensation in glaucoma. *Invest Ophthalmol Vis Sci* 2003;44:2606-12.
16. Shirakashi M, Yaeoda K, Fukushima A, Funaki S, Funaki H, Ofuchi N, *et al.* Usefulness of GDx VCC in glaucoma detection. *J Eye* 2003;20:1019-21.
17. Greenfield DS, Knighton RW, Huang XR. Effect of corneal polarization axis on assessment of retinal nerve fiber layer thickness by scanning laser polarimetry. *Am J Ophthalmol* 2000;129:715-22.

18. Bowd C, Zangwill LM, Weinreb RN. Association between scanning laser polarimetry measurements using variable corneal polarization compensation and visual field sensitivity in glaucomatous eyes. *Arch Ophthalmol* 2003;121:961-6.
19. Saito H, Tomidokoro A, Yanagisawa M, Aihara M, Tomita G, Araie M. Scanning laser polarimetry with enhanced corneal compensation in patients with open-angle glaucoma. *J Glaucoma* 2008;17:24-9.
20. Medeiros FA, Bowd C, Zangwill LM, Patel C, Weinreb RN. Detection of glaucoma using scanning laser polarimetry with enhanced corneal compensation. *Invest Ophthalmol Vis Sci* 2007;48:3146-53.
21. Dada T, Gadia R, Aggarwal A, Dave V, Gupta V, Sihota R. Retinal nerve fiber layer thickness measurement by scanning laser polarimetry (GDxVCC) at conventional and modified diameter scans in normals, glaucoma suspects, and early glaucoma patients. *J Glaucoma* 2009;18:448-52.
22. Bagga H, Greenfield DS, Feuer W, Knighton RW. Scanning laser polarimetry with variable corneal compensation and optical coherence tomography in normal and glaucomatous eyes. *Am J Ophthalmol* 2003;135:521-9.
23. Schlottmann PG, De Cilla S, Greenfield DS, Caprioli J, Garway-Heath DF. Relationship between visual field sensitivity and retinal nerve fiber layer thickness as measured by scanning laser polarimetry. *Invest Ophthalmol Vis Sci* 2004;45:1823-9.
24. Reus NJ, Lemij HG. Scanning laser polarimetry of the retinal nerve fiber layer in perimetrically unaffected eyes of glaucoma patients. *Ophthalmology* 2004;111:2199-203.
25. Choplin NT, Zhou Q, Knighton RW. Effect of individualized compensation for anterior segment birefringence on retinal nerve fiber layer assessments as determined by scanning laser polarimetry. *Ophthalmology* 2003;110:719-25.
26. Langlotz CP. Fundamental measures of diagnostic examination performance: Usefulness for clinical decision making and research. *Radiology* 2003;228:3-9.
27. Sanchez-Galeana C, Bowd C, Blumenthal EZ, Gokhale PA, Zangwill LM, Weinreb RN. Using optical imaging summary data to detect glaucoma. *Ophthalmology* 2001;108:1812-8.
28. Rao HL, Venkatesh CR, Vidyasagar K, Yadav RK, Addepalli UK, Jude A, *et al.* Retinal nerve fiber Layer measurements by scanning laser Polarimetry with enhanced corneal compensation in healthy subjects. *J Glaucoma* 2013.
29. Medeiros FA, Vizzeri G, Zangwill LM, Alencar LM, Sample PA, Weinreb RN. Comparison of retinal nerve fiber layer and optic disc imaging for diagnosing glaucoma in patients suspected of having the disease. *Ophthalmology* 2008;115:1340-6.
30. Mohammadi K, Bowd C, Weinreb RN, Medeiros FA, Sample PA, Zangwill LM. Retinal nerve fiber layer thickness measurements with scanning laser polarimetry predict glaucomatous visual field loss. *Am J Ophthalmol* 2004;138:592-601.
31. Badalà F, Nouri-Mahdavi K, Raof DA, Leeprechanon N, Law SK, Caprioli J. Optic disk and nerve fiber layer imaging to detect glaucoma. *Am J Ophthalmol* 2007;144:724-32.
32. Shaikh A, Salmon JF. The role of scanning laser polarimetry using the GDx variable corneal compensator in the management of glaucoma suspects. *Br J Ophthalmol* 2006;90:1454-7.
33. Li G, Fansi AK, Harasymowycz P. Screening for glaucoma using GDx-VCC in a population with=1 risk factors. *Can J Ophthalmol* 2013;48:279-85.
34. Benítez-del-Castillo J, Martínez A, Regi T. Correlation between scanning laser polarimetry with and without enhanced corneal compensation and high-definition optical coherence tomography in normal and glaucomatous eyes. *Int J Clin Pract* 2011;65:807-16.
35. Zheng W, Baohua C, Qun C, Zhi Q, Hong D. Retinal nerve fiber layer images captured by GDx-VCC in early diagnosis of glaucoma. *Ophthalmologica* 2008;222:17-20.
36. Da Pozzo S, Fuser M, Vattovani O, Di Stefano G, Ravalico G. GDx-VCC performance in discriminating normal from glaucomatous eyes with early visual field loss. *Graefes Arch Clin Exp Ophthalmol* 2006;244:689-95.
37. Parikh RS, Parikh SR, Kumar RS, Prabakaran S, Babu JG, Thomas R. Diagnostic capability of scanning laser polarimetry with variable cornea compensator in Indian patients with early primary open-angle glaucoma. *Ophthalmology* 2008;115:1167-1172.e1.
38. Fortune B, Burgoyne CF, Cull G, Reynaud J, Wang L. Onset and progression of peripapillary retinal nerve fiber layer (RNFL) retardance changes occur earlier than RNFL thickness changes in experimental glaucoma. *Invest Ophthalmol Vis Sci* 2013;54:5653-61.
39. Reus NJ, Lemij HG. Diagnostic accuracy of the GDx VCC for glaucoma. *Ophthalmology* 2004;111:1860-5.
40. Henderson PA, Medeiros FA, Zangwill LM, Weinreb RN. Relationship between central corneal thickness and retinal nerve fiber layer thickness in ocular hypertensive patients. *Ophthalmology* 2005;112:251-6.
41. Choi J, Cho HS, Lee CH, Kook MS. Scanning laser polarimetry with variable corneal compensation in the area of apparently normal hemifield in eyes with normal-tension glaucoma. *Ophthalmology* 2006;113:1954-60.
42. Jung JI, Kim JH, Kook MS. Comparison of retinal nerve fiber layer measurements between NTG and HTG using GDx-VCC. *Korean J Ophthalmol* 2006;20:26-32.
43. Zareii R, Soleimani M, Moghimi S, Eslami Y, Fakhraie G, Amini H. Relationship between GDx VCC and Stratus OCT in juvenile glaucoma. *Eye (Lond)* 2009;23:2182-6.
44. Dimopoulos AT, Katsanos A, Mikropoulos DG, Giannopoulos T, Empeslidis T, Teus MA, *et al.* Scanning laser polarimetry in eyes with exfoliation syndrome. *Eur J Ophthalmol* 2013;23:743-50.
45. Tóth M, Holló G. Enhanced corneal compensation for scanning laser polarimetry on eyes with atypical polarisation pattern. *Br J Ophthalmol* 2005;89:1139-42.
46. Da Pozzo S, Marchesan R, Canziani T, Vattovani O, Ravalico G. Atypical pattern of retardation on GDx-VCC and its effect on retinal nerve fibre layer evaluation in glaucomatous eyes. *Eye (Lond)* 2006;20:769-75.
47. Bagga H, Greenfield DS, Feuer WJ. Quantitative assessment of atypical birefringence images using scanning laser polarimetry with variable corneal compensation. *Am J Ophthalmol* 2005;139:437-46.
48. Mai TA, Reus NJ, Lemij HG. Diagnostic accuracy of scanning laser polarimetry with enhanced versus variable corneal compensation. *Ophthalmology* 2007;114:1988-93.
49. Orlev A, Horani A, Rapson Y, Cohen MJ, Blumenthal EZ. Clinical characteristics of eyes demonstrating atypical patterns in scanning laser polarimetry. *Eye (Lond)* 2008;22:1378-83.
50. Reus NJ, Zhou Q, Lemij HG. Enhanced imaging algorithm for scanning laser polarimetry with variable corneal compensation. *Invest Ophthalmol Vis Sci* 2006;47:3870-7.
51. Tóth M, Holló G. Evaluation of enhanced corneal compensation in scanning laser polarimetry: Comparison with variable corneal compensation on human eyes undergoing LASIK. *J Glaucoma* 2006;15:53-9.
52. Bowd C, Tavares IM, Medeiros FA, Zangwill LM, Sample PA, Weinreb RN. Retinal nerve fiber layer thickness and visual sensitivity using scanning laser polarimetry with variable and enhanced corneal compensation. *Ophthalmology* 2007;114:1259-65.
53. Hoel LM, Tornow RP, Schrems WA, Horn FK, Mardin CY, Kruse FE, *et al.* Glaucoma diagnostic performance of GDxVCC and spectralis OCT on eyes with atypical retardation pattern. *J Glaucoma* 2013;22:317-24.

54. Wang Z, Liu XW, Li XY, Zhang WJ, Dai H. Detection of the changes of retinal nerve fiber layer thickness by GDx-VCC laser scanning polarimetry in primary open angle glaucoma patients. *Zhonghua Yan Ke Za Zhi* 2012;48:497-501.
55. Medeiros FA, Zangwill LM, Alencar LM, Sample PA, Weinreb RN. Rates of progressive retinal nerve fiber layer loss in glaucoma measured by scanning laser polarimetry. *Am J Ophthalmol* 2010;149:908-15.
56. Makabe K, Takei K, Oshika T. Longitudinal relationship between retinal nerve fiber layer thickness parameters assessed by scanning laser polarimetry (GDxVCC) and visual field in glaucoma. *Graefes Arch Clin Exp Ophthalmol* 2012;250:575-81.
57. Vetrugno M, Trabucchi T, Sisto D, Sborgia C. Effect of cataract surgery and foldable intraocular lens implantation on retinal nerve fiber layer as measured by scanning laser polarimetry with variable corneal compensator. *Eur J Ophthalmol* 2004;14:106-10.
58. Park RJ, Chen PP, Karyampudi P, Mills RP, Harrison DA, Kim J. Effects of cataract extraction with intraocular lens placement on scanning laser polarimetry of the peripapillary nerve fiber layer. *Am J Ophthalmol* 2001;132:507-11.
59. Iacono P, Da Pozzo S, Vattovani O, Tognetto D, Ravalico G. Scanning laser polarimetry of nerve fiber layer thickness in normal eyes after cataract phacoemulsification and foldable intraocular lens implantation. *J Cataract Refract Surg* 2005;31:1042-9.
60. Dada T, Behera G, Agarwal A, Kumar S, Sihota R, Panda A. Effect of cataract surgery on retinal nerve fiber layer thickness parameters using scanning laser polarimetry (GDxVCC). *Indian J Ophthalmol* 2010;58:389-94.
61. Gazzard G, Foster PJ, Devereux JG, Oen F, Chew PT, Khaw PT, *et al.* Effect of cataract extraction and intraocular lens implantation on nerve fibre layer thickness measurements by scanning laser polarimeter (GDx) in glaucoma patients. *Eye (Lond)* 2004;18:163-8.
62. Brittain CJ, Fong KC, Hull CC, Gillespie IH. Changes in scanning laser polarimetry before and after laser capsulotomy for posterior capsular opacification. *J Glaucoma* 2007;16:112-6.
63. Dada T, Chaudhary S, Muralidhar R, Nair S, Sihota R, Vajpayee RB. Evaluation of retinal nerve fiber layer thickness measurement following laser *in situ* keratomileusis using scanning laser polarimetry. *Indian J Ophthalmol* 2007;55:191-4.
64. Zangwill LM, Abunto T, Bowd C, Angeles R, Schanzlin DJ, Weinreb RN. Scanning laser polarimetry retinal nerve fiber layer thickness measurements after LASIK. *Ophthalmology* 2005;112:200-7.
65. Katsanos A, Kóthy P, Nagy ZZ, Holló G. Scanning laser polarimetry of retinal nerve fibre layer thickness after laser assisted *in situ* keratomileusis (LASIK): Stability of the values after the third post-LASIK month. *Acta Physiol Hung* 2004;91:119-30.
66. Leung CK, Chan WM, Chong KK, Yung WH, Tang KT, Woo J, *et al.* Comparative study of retinal nerve fiber layer measurement by StratusOCT and GDx VCC, I: Correlation analysis in glaucoma. *Invest Ophthalmol Vis Sci* 2005;46:3214-20.
67. Chung YS, Sohn YH. The relationship between optical coherence tomography and scanning laser polarimetry measurements in glaucoma. *Korean J Ophthalmol* 2006;20:225-9.
68. Kim HG, Heo H, Park SW. Comparison of scanning laser polarimetry and optical coherence tomography in preperimetric glaucoma. *Optom Vis Sci* 2011;88:124-9.
69. Yoo YC, Park KH. Comparison of optical coherence tomography and scanning laser polarimetry for detection of localized retinal nerve fiber layer defects. *J Glaucoma* 2010;19:229-36.
70. Aptel F, Sayous R, Fortoul V, Beccat S, Denis P. Structure-function relationships using spectral-domain optical coherence tomography: Comparison with scanning laser polarimetry. *Am J Ophthalmol* 2010;150:825-33.
71. Lee S, Sung KR, Cho JW, Cheon MH, Kang SY, Kook MS. Spectral-domain optical coherence tomography and scanning laser polarimetry in glaucoma diagnosis. *Jpn J Ophthalmol* 2010;54:544-9.
72. Xu G, Weinreb RN, Leung CK. Retinal nerve fiber layer progression in glaucoma: A comparison between retinal nerve fiber layer thickness and retardance. *Ophthalmology* 2013;120:2493-500.
73. Sehi M, Ume S, Greenfield DS. Scanning laser polarimetry with enhanced corneal compensation and optical coherence tomography in normal and glaucomatous eyes. *Invest Ophthalmol Vis Sci* 2007;48:2099-104.
74. Garas A, Vargha P, Holló G. Comparison of diagnostic accuracy of the RTVue Fourier-domain OCT and the GDx-VCC/ECC polarimeter to detect glaucoma. *Eur J Ophthalmol* 2012;22:45-54.
75. Schallenberg M, Dekowski D, Kremmer S, Selbach JM, Steuhl KP. Comparison of Spectralis-OCT, GDxVCC and GDxECC in assessing retinal nerve fiber layer (RNFL) in glaucomatous patients. *Graefes Arch Clin Exp Ophthalmol* 2013;251:1343-53.
76. Jansonius NM, Heeg GP. The Groningen Longitudinal Glaucoma Study. II. A prospective comparison of frequency doubling perimetry, the GDx nerve fibre analyser and standard automated perimetry in glaucoma suspect patients. *Acta Ophthalmol* 2009;87:429-32.
77. Alencar LM, Zangwill LM, Weinreb RN, Bowd C, Sample PA, Girkin CA, *et al.* A comparison of rates of change in neuroretinal rim area and retinal nerve fiber layer thickness in progressive glaucoma. *Invest Ophthalmol Vis Sci* 2010;51:3531-9.
78. Kanamori A, Nagai-Kusuhara A, Escaño MF, Maeda H, Nakamura M, Negi A. Comparison of confocal scanning laser ophthalmoscopy, scanning laser polarimetry and optical coherence tomography to discriminate ocular hypertension and glaucoma at an early stage. *Graefes Arch Clin Exp Ophthalmol* 2006;244:58-68.
79. Medeiros FA, Zangwill LM, Bowd C, Weinreb RN. Comparison of the GDx VCC scanning laser polarimeter, HRT II confocal scanning laser ophthalmoscope, and stratus OCT optical coherence tomograph for the detection of glaucoma. *Arch Ophthalmol* 2004;122:827-37.
80. Hong S, Ahn H, Ha SJ, Yeom HY, Seong GJ, Hong YJ. Early glaucoma detection using the Humphrey Matrix Perimeter, GDx VCC, Stratus OCT, and retinal nerve fiber layer photography. *Ophthalmology* 2007;114:210-5.
81. Kunimatsu S, Tomidokoro A, Saito H, Aihara M, Tomita G, Araie M. Performance of GDx VCC in eyes with peripapillary atrophy: Comparison of three circle sizes. *Eye (Lond)* 2008;22:173-8.
82. Wang G, Qiu KL, Lu XH, Sun LX, Liao XJ, Chen HL, *et al.* The effect of myopia on retinal nerve fibre layer measurement: A comparative study of spectral-domain optical coherence tomography and scanning laser polarimetry. *Br J Ophthalmol* 2011;95:255-60.
83. Wang Z, Liu XW, Li XY, Zhang WJ, Dai H. Detection of the changes of retinal nerve fiber layer thickness by GDx-VCC laser scanning polarimetry in primary open angle glaucoma patients. *Zhonghua Yan Ke Za Zhi* 2012;48:497-501.
84. Dada T, Aggarwal A, Bali SJ, Sharma A, Shah BM, Angmo D, *et al.* Evaluation of retinal nerve fiber layer thickness parameters in myopic population using scanning laser polarimetry (GDxVCC). *Nepal J Ophthalmol* 2013;5:3-8.
85. Yu S, Tanabe T, Hangai M, Morishita S, Kurimoto Y, Yoshimura N. Scanning laser polarimetry with variable corneal compensation and optical coherence tomography in tilted disk. *Am J Ophthalmol* 2006;142:475-82.
86. Bozkurt B, Irkeç M, Tatlipinar S, Erdener U, Orhan M, Gedik S, *et al.* Retinal nerve fiber layer analysis and interpretation of GDx

- parameters in patients with tilted disc syndrome. *Int Ophthalmol* 2001;24:27-31.
87. Bagga H, Greenfield DS, Knighton RW. Scanning laser polarimetry with variable corneal compensation: Identification and correction for corneal birefringence in eyes with macular disease. *Invest Ophthalmol Vis Sci* 2003;44:1969-76.
88. Dada T, Tinwala SI, Dave V, Agarwal A, Sharma R, Wadhvani M. Effect of change in macular birefringence imaging protocol on retinal nerve fiber layer thickness parameters using GDx VCC in eyes with macular lesions. *Int Ophthalmol* 2014;34:901-7.

Cite this article as: Dada T, Sharma R, Angmo D, Sinha G, Bhartiya S, Mishra SK, *et al.* Scanning laser polarimetry in glaucoma. *Indian J Ophthalmol* 2014;62:1045-55.

Source of Support: Nil. **Conflict of Interest:** None declared.